

Positron-helium collisions: Positronium formation using the distorted-wave approximation

Subhrangsu Sen* and Puspajit Mandal

Department of Mathematics, Visva-Bharati University, Santiniketan, District Birbhum, 731 235 West Bengal, India

(Received 1 August 2009; revised manuscript received 7 November 2009; published 10 December 2009)

Accurate Hylleraas-type correlated helium wave functions are used to predict positronium (Ps) formation cross sections in positron-helium collisions within the frame work of the distorted-wave approximation at intermediate and high energies of positron impact. Exponential correlated atomic target wave functions taking into account up to $N=30$ basis terms are utilized. Reliable total cross sections for the ground and excited $2s$ -state Ps formation are reported at intermediate and high energies. The present distorted-wave results are in conformity with the existing theoretical and experimental values available in the literature for intermediate and high-energy positrons. Surface plots of the DWA differential cross section reveal rich structures due to constructive and destructive interference between angular momentum states of the moving Ps.

DOI: [10.1103/PhysRevA.80.062714](https://doi.org/10.1103/PhysRevA.80.062714)

PACS number(s): 34.70.+e, 34.80.Uv

I. INTRODUCTION

Over the last few decades positron scattering physics has been an active area of interest both theoretically and experimentally because of its wide applications in different branches of physics, chemistry, and other fields [1–6]. Also positron scattering from atoms and molecules is very much different from the corresponding case of electron scattering in that the static interaction for positrons is repulsive while for electrons it is attractive. The dipole polarization in both cases however is attractive in nature. Thus, for positron-atom and positron-molecule collisions the results are heavily dependent on the degree of cancellation of the static and polarization interactions. Another important difference compared with electron scattering is the absence of exchange interaction in the positron scattering case. Additionally there arises the possibility of charge transfer in positron-atom and positron-molecule collisions leading to positronium (Ps) formation the study of which becomes much more complicated theoretically due to change of coordinates in the entrance and outgoing channels. Normally during scattering of positrons by an atom, such as hydrogen, helium, argon, neon, xenon, krypton, etc, the Ps formation channel opens up below the first excitation threshold of the atom. However, in the case of positron-alkali-atom collisions, the Ps formation can occur even for zero energy positrons as the outer electron of the alkali atom is very loosely bound.

The perfect three-body problem of Ps formation during positron-hydrogen collisions, $e^+ + (e^- + H^+) \rightarrow (e^+e^-)(1s) + H^+$, has drawn the attention of a huge number of theoretical and experimental workers [7–11] in the past with the result that it is now considered to be solved at least in the Oré gap, 6.8–10.2 eV. A large variety of approximations have been used in these works and a wide range of collision processes, such as, excitations, ionizations, electron transfer to continuum (ECC) etc has been studied with definitive results. Very sophisticated and challenging experiments have also been carried out simultaneously at different laboratories and new lights have been shed to understand some of the fundamental properties of nature involving positrons.

Ps formation during the collision process, $e^+ + \text{He}(1s^2) \rightarrow (e^+e^-)(1s) + \text{He}^+(1s)$, is an example of a fundamental rearrangement collision involving two active electrons in the target atom. However in the case of helium, the situation is not similar to that for the positron-hydrogen system. One reason for this seems to be that the two-electron helium states are not exactly known. A perfect calculation for Ps formation during passage of positrons through helium is indeed very difficult and complicated.

In a pioneering work in 1954, Massey and Mohr [12] made an estimate of the cross section for Ps formation in positron-hydrogen collisions using the first Born approximation (FBA) and the distorted-wave approximation (DWA). The first theoretical prediction for Ps formation in helium was performed by Massey and Moussa [13] in 1961 using the FBA. These authors wrote down the scattering equations within the frame work of the two-state close-coupling approximation (CCA) considering elastic scattering and Ps formation only. They reported the total Ps formation cross section at several incident positron energies from the threshold up to 125 eV with the use of the simplest Hylleraas helium wave function. Both for hydrogen and helium as targets, the total Ps formation cross section displayed similar nature. Rising sharply from the threshold to a peak value it fell off smoothly with the increase of incident energy.

Over the years the problem attracted the fancy of a large number of theoretical workers. A wide variety of approximations with various degrees of sophistication have been used to investigate this rearrangement scattering process.

Humberston and co-workers [14] performed the most elaborate and sophisticated calculations to date on elastic scattering and Ps formation during positron-helium collisions at low energies from the threshold at 17.8–24 eV. They solved the problem using the Kohn and Inverse-Kohn variational principles for only a few partial waves. In their calculations, they included quite a number of linear terms in the scattering basis functions and used fairly accurate correlated Hylleraas-type wave functions involving 5, 12, and 22 linear terms. Among other things their investigations revealed that there were striking similarities in the behavior of s -wave cross sections for Ps formation in positron-H and positron-He collisions at low energies. Their studies also reveal the threshold behavior of the Ps formation cross section.

*Also at Patha-Bhavana, Visva-Bharati University.

Mandal *et al.* [15] used a two-state CCA to consider elastic scattering and Ps(1s) formation in positron-He collisions and reported cross sections at low energies for only a few partial waves. Later Mandal *et al.* [16] used the DWA to study Ps(1s) formation in positron-helium collisions and the FBA to study Ps(ns) formation at intermediate and high energies. The DWA was subsequently used by Khan and Ghosh [17] and Khan *et al.* [18] to investigate the problem at low and intermediate energies.

Bransden and co-workers [19] investigated positron-helium collisions employing the CCA in the momentum space to calculate Ps formation in 1s, 2s, 2p states, and helium excitation processes 1^1S-2^1S and 2^1P at energies between 31.3 and 200 eV. They used an independent electron model combined with a model potential to represent the helium atom. Their findings indicate that the 2^1S - and 2^1P -excitation cross sections are reduced due to Ps formation. The calculated total Ps formation cross sections are in agreement with the experimental data below 100 eV.

Campbell *et al.* [20] used a sophisticated CCA with the inclusion of a large number of basis states and pseudostates. Wu *et al.* [21] performed also a very reliable calculation using the single-centered convergent close-coupling (CCC) method with two different models for the target structure at incident energies in the range from the ionization threshold to 1 keV. In one model CCC(FC) the target structure was constructed with the frozen core approximation, while in the other model CCC(MC), the target helium ground state was represented in the multiconfiguration expansion. In these two close-coupling calculations, the target continuum and rearrangement channels have been explicitly included by employing pseudostates. The predicted results are in close agreement with the observed data.

Other methods used to study Ps formation in helium were classical trajectory Monte-Carlo (CTMC) technique by Schulz *et al.* [22], the target continuum distorted-wave approximation (TCDWA) by Deb *et al.* [23], and the hyperspherical coupled-channel method by Igarashi and Toshima [24] with an independent electron approximation. The Ps formation cross sections due to these theoretical investigations are in overall agreement with the observed values at different ranges of incident positron energy.

Very recently a number of theoretical calculations have been reported on the positron-helium system by Zhou and co-workers [25], in which the authors used the momentum-space coupled-channel optical (CCO) model to estimate elastic, excitation, Ps formation, and ionization cross sections at intermediate and high energies. Their predicted total cross sections are in satisfactory agreement with the experimental data.

Due to technological advancement during the past three decades, quite a number of exciting experimental observations have been made at different centers on many aspects of positron collision physics. Among these mention may be made of the experiments performed on the positron-helium system by Kauppila *et al.* [26], Charlton *et al.* [27], Fornari *et al.* [28], Fromme *et al.* [29], Murtagh *et al.* [30], Overton *et al.* [31], etc.

It is relevant at this point to mention that, except for the variational calculations by the University College London

group of Humberston and co-workers [14], in almost all of these theoretical studies two-electron correlated wave functions for helium have *not* been used. Simplest Hylleraas and Hartree-Fock wave functions of helium have mainly been utilized.

We have initiated investigations, in which it is our main objective to study systematically the effect of correlated wave functions in positron-helium collisions. As there are limited number of investigations on the differential cross section in the literature, it would be our intention to concentrate our focus and attention to a detailed study on the various aspects and nature of this rearrangement scattering problem.

In the present calculation on Ps formation, we have used highly accurate Hylleraas-type correlated helium wave functions of Kar and Ho [32] within the framework of the distorted-wave theory as developed recently by Ghoshal and Mandal [33]. Because of its exponential form, we have been able to incorporate the wave function very conveniently in our scattering formulation. Indeed we have increased systematically the number of correlation terms and have determined the Ps formation cross sections in positron-helium collisions with unto $N=30$ basis terms.

Our findings indicate that there is a general trend of convergence in the Ps formation cross section values with respect to the increase of number of correlation terms in the target helium wave function. It thus seems to be a comprehensive study on Ps formation in positron-helium collisions using a fairly decent distorted-wave model. Making use of a huge set of data arising out of this investigation, useful conclusions are made on the differential and total cross sections at intermediate and high incident energies.

The plan of the paper is as follows. In Sec. II, we discuss very briefly the formulation of the distorted-wave theory and present our results in Sec. III. The concluding remarks are made in Sec. IV. We use atomic units in our calculations in which $a_0=m_e=m_p=e=\hbar=1$.

II. THEORY

We denote by \mathbf{r}_0 the position vector of the incident positron and by $\mathbf{r}_1, \mathbf{r}_2$, those of the atomic electrons 1 and 2 relative to the atomic nucleus, which is assumed to be infinitely heavy and at rest at the origin. The relative coordinate, $\mathbf{r}_{10}=\mathbf{r}_1-\mathbf{r}_0$, and the center of mass coordinate, $\mathbf{s}_{10}=\frac{1}{2}(\mathbf{r}_1+\mathbf{r}_0)$, refer, respectively, to the bound states of the Ps and the moving Ps relative to the origin involving the positron and the atomic electron 1, while the other electron 2 remains attached to the nucleus as a spectator in the bound states of $\text{He}^+(nlm)$. In our calculation we have considered only the ground state of $\text{He}^+(100)$.

The full Hamiltonian of the positron-helium system may be expressed as $H=H_i+V_i=H_f+V_f$, where the Hamiltonian in the entrance channel is denoted by H_i and the final channel Hamiltonian by H_f and V_i and V_f are the residual interactions in the incident and the final channel, respectively, which are usually referred to as the 'prior' and 'post' interactions.

The plane-wave states Φ_i and Φ_f corresponding to the Hamiltonians H_i and H_f satisfy $H_i\Phi_i=E_i\Phi_i$ and $H_f\Phi_f=E_f\Phi_f$, where E_i and E_f denote the total energies in the in-

cident and final channels. The energy conservation requires that $E_i = E_f = E$ = the total energy of the system.

The Ps formation amplitude in positron-helium collisions within the framework of the second-order DWA is obtained as [33]

$$g_{\text{DWA}}(\mathbf{k}_f, \mathbf{k}_i) = -\frac{\mu_f}{2\pi} \langle \chi_f^- | V_f - U_f | \chi_i^+ \rangle, \quad (1)$$

in which the distorted waves χ_i^+ and χ_f^- in the entrance and final channel, respectively, are given by

$$\chi_i^+ = \Phi_i + G_i^+ U_i \Phi_i, \quad \chi_f^- = \Phi_f + G_f^- U_f \Phi_f, \quad (2)$$

where G_i^+ and G_f^- are the Green's operators, and U_i and U_f are the average interactions in the entrance and exit channels, and the reduced mass $\mu_f = 2$.

For positron-H and positron-He collisions, we find that $U_f = 0$ (see the Appendix). Thus, on using Eq. (2) in Eq. (1), we obtain

$$g_{\text{DWA}}(\mathbf{k}_f, \mathbf{k}_i) = -\frac{\mu_f}{2\pi} \langle \Phi_f | V_f | \Phi_i + G_i^+ U_i \Phi_i \rangle, \quad (3)$$

which may be written as

$$g_{\text{DWA}}(\mathbf{k}_f, \mathbf{k}_i) = g_B(\mathbf{k}_f, \mathbf{k}_i) + g_D(\mathbf{k}_f, \mathbf{k}_i), \quad (4)$$

where the amplitude in the FBA is given as

$$g_B(\mathbf{k}_f, \mathbf{k}_i) = -\frac{\mu_f}{2\pi} \langle \Phi_f | V_f | \Phi_i \rangle, \quad (5)$$

and the second-order distorted-wave correction amplitude as

$$g_D(\mathbf{k}_f, \mathbf{k}_i) = -\frac{\mu_f}{2\pi} \langle \Phi_f | V_f G_i^+ U_i | \Phi_i \rangle, \quad (6)$$

in which the post interaction V_f in a.u. is

$$V_f = \frac{Z}{r_0} - \frac{Z}{r_1} + \frac{1}{r_{12}} - \frac{1}{r_{02}}, \quad (7)$$

and the static interaction U_i in the entrance channel is

$$U_i = \int |\phi_i(\mathbf{r}_1, \mathbf{r}_2)|^2 V_i d\mathbf{r}_1 d\mathbf{r}_2, \quad (8)$$

with the prior interaction V_i in a.u. given by

$$V_i = \frac{Z}{r_0} - \frac{1}{r_{01}} - \frac{1}{r_{02}}. \quad (9)$$

The forms of the exponential correlated two-electron helium states $\phi_i(\mathbf{r}_1, \mathbf{r}_2)$ as proposed by Kar and Ho [32] and used in the present calculations are given as:

$$\begin{aligned} \phi_i(\mathbf{r}_1, \mathbf{r}_2) = \frac{1}{\sqrt{2}} \sum_{i=1}^N C_i [\exp(-\alpha_i r_1 - \beta_i r_2 - \gamma_i r_{12}) \\ + \exp(-\beta_i r_1 - \alpha_i r_2 - \gamma_i r_{12})], \end{aligned} \quad (10)$$

with

$$\alpha_i = \eta [\langle \langle i(i+1)/\sqrt{2} \rangle \rangle (A_2 - A_1) + A_1],$$

$$\beta_i = \eta [\langle \langle i(i+1)/\sqrt{2} \rangle \rangle (B_2 - B_1) + B_1],$$

$$\gamma_i = \eta [\langle \langle i(i+1)/\sqrt{2} \rangle \rangle (C_2 - C_1) + C_1],$$

where the symbol $\langle \langle \dots \rangle \rangle$ denotes the fractional part of a real number. The pseudorandom numbers, $A_i, B_i, C_i (i=1, 2)$ and the real parameter η are chosen to optimize the eigenenergy within the framework of the Raleigh-Ritz variational principle. These wave functions predict very accurate values of the eigenenergy and the dipole polarizability.

In this calculation we have taken into consideration the effect of dipole polarization in the incident channel by a simple “parameter-free” Buckingham potential:

$$V_p = -\frac{\alpha}{(r_0^2 + r_c^2)^2}, \quad (11)$$

where $\alpha = 1.38(a_0^3)$ is the dipole polarizability of helium, and r_c is the cutoff parameter taken equal to 1. The elastic scattering amplitude is, thus, modified by this potential to give the polarized Born amplitude.

III. RESULTS AND DISCUSSIONS

In this paper, we discuss mainly the total cross sections for Ps(1s) and Ps(2s) formations during positron scattering from normal helium in the incident energy range 30–500 eV. Results within the frame works of FBA and DWA using correlated helium ground state with $N=2, 4, 6$, and 30 basis terms are computed in this calculation. Computations have also been carried out using the HF wave function of helium for Ps(1s) formation. The FBA results are however not discussed here in detail. The present results are compared with the theoretical predictions and experimental observations available in the literature.

A. DWA cross sections

The DWA total cross sections have been computed for Ps(1s) and Ps(2s) formations in the incident energy range of 30–500 eV and are shown in Table I. As for FBA, these cross sections are also calculated for the same number of basis terms $N=2, 4, 6$, and 30 in the correlated helium-wave function. This table also includes the DWA values of Ps(1s) formation for the HF wave function.

The present calculations reveal that the values of the cross section for basis terms $N=2$ are much larger than those for higher basis terms. There is however a broad systematic agreement between the cross sections for $N=4, 6$, and 30 terms at all incident energies. It therefore seems that higher number of basis terms in the correlated wave function is in

TABLE I. Total Ps formation cross sections in $1s$ and $2s$ states (in units of πa_0^2) in positron-helium collisions using DWA with Hartree-Fock (HF) for $1s$ and correlated wave functions having $N=2,4,6,30$ basis terms both for $1s$ and $2s$ states. The notation $x[\pm y]$ stands for $x \times 10^{\pm y}$.

E (eV)	HF	$N=2$		$N=4$		$N=6$		$N=30$	
	$\sigma_{Ps}^{DWA}(1s)$	$\sigma_{Ps}^{DWA}(1s)$	$\sigma_{Ps}^{DWA}(2s)$	$\sigma_{Ps}^{DWA}(1s)$	$\sigma_{Ps}^{DWA}(2s)$	$\sigma_{Ps}^{DWA}(1s)$	$\sigma_{Ps}^{DWA}(2s)$	$\sigma_{Ps}^{DWA}(1s)$	$\sigma_{Ps}^{DWA}(2s)$
30	0.2852	0.3037	0.2413[−1]	0.2828	0.1327[−1]	0.2791	0.1303[−1]	0.2825	0.1420[−1]
40	0.3136	0.2005	0.1916[−1]	0.3226	0.2500[−1]	0.3120	0.2443[−1]	0.3084	0.2404[−1]
50	0.2820	0.1577	0.1669[−1]	0.2930	0.2916[−1]	0.2824	0.2836[−1]	0.2766	0.2751[−1]
60	0.2290	0.1261	0.1406[−1]	0.2387	0.2632[−1]	0.2300	0.2553[−1]	0.2240	0.2465[−1]
70	0.1787	0.1001	0.1169[−1]	0.1863	0.2200[−1]	0.1797	0.2131[−1]	0.1742	0.2051[−1]
80	0.1376	0.7903[−1]	0.9770[−2]	0.1434	0.1808[−1]	0.1385	0.1752[−1]	0.1337	0.1679[−1]
90	0.1059	0.6245[−1]	0.8155[−2]	0.1102	0.1469[−1]	0.1066	0.1425[−1]	0.1026	0.1361[−1]
100	0.8193[−1]	0.4952[−1]	0.6738[−2]	0.8506[−1]	0.1181[−1]	0.8246[−1]	0.1146[−1]	0.7915[−1]	0.1092[−1]
110	0.6390[−1]	0.3951[−1]	0.5517[−2]	0.6618[−1]	0.9417[−2]	0.6427[−1]	0.9145[−2]	0.6156[−1]	0.8701[−2]
120	0.5030[−1]	0.3174[−1]	0.4499[−2]	0.5195[−1]	0.7494[−2]	0.5054[−1]	0.7284[−2]	0.4834[−1]	0.6920[−2]
150	0.2596[−1]	0.1722[−1]	0.2483[−2]	0.2658[−1]	0.3879[−2]	0.2598[−1]	0.3780[−2]	0.2479[−1]	0.3585[−2]
200	0.1020[−1]	0.7189[−2]	0.1061[−2]	0.1028[−1]	0.1525[−2]	0.1012[−1]	0.1494[−2]	0.9660[−2]	0.1419[−2]
250	0.4711[−2]	0.3469[−2]	0.5374[−3]	0.4683[−2]	0.7256[−3]	0.4629[−2]	0.7145[−3]	0.4434[−2]	0.6821[−3]
300	0.2445[−2]	0.1863[−2]	0.3063[−3]	0.2403[−2]	0.3938[−3]	0.2382[−2]	0.3893[−3]	0.2291[−2]	0.3738[−3]
350	0.1383[−2]	0.1083[−2]	0.1880[−3]	0.1346[−2]	0.2327[−3]	0.1337[−2]	0.2306[−3]	0.1291[−2]	0.2227[−3]
400	0.8345[−3]	0.6684[−3]	0.1210[−3]	0.8066[−3]	0.1455[−3]	0.8022[−3]	0.1445[−3]	0.7771[−3]	0.1401[−3]
450	0.5297[−3]	0.4323[−3]	0.8054[−4]	0.5091[−3]	0.9474[−4]	0.5067[−3]	0.9420[−4]	0.4923[−3]	0.9164[−4]
500	0.3500[−3]	0.2903[−3]	0.5505[−4]	0.3349[−3]	0.6364[−4]	0.3335[−3]	0.6334[−4]	0.3248[−3]	0.6178[−4]

fact required to obtain consistently reliable Ps formation cross sections.

In Table II, we compare our predictions with the theoretical data of Mandal *et al.* [16], Khan *et al.* [17,18] and Hewitt *et al.* [19]. In this table, we have included our Ps($1s$) cross sections using HF wave function as well as correlated wave function with $N=30$ terms. The Ps($2s$) cross sections reported here are calculated with $N=30$ terms only. The

present results compare well with those of Khan *et al.* [17,18], and are consistent with the other theoretical values at intermediate and high energies.

For comparison with the existing theoretical and experimental results, we have displayed the values of the DWA total cross sections for Ps formation ($1s+2s+2p$) in Figs. 1 and 2. While drawing the figure, we have followed the suggestions of Hewitt *et al.* [19] in that the Ps($1s$) cross section

TABLE II. Comparison of total Ps formation cross sections in $1s$ and $2s$ states (in units of πa_0^2) in positron-helium collisions using DWA with Hartree-Fock (HF) for $1s$ and correlated wave functions having $N=30$ basis terms both for $1s$ and $2s$ states with available theoretical results. The notation $x[\pm y]$ stands for $x \times 10^{\pm y}$.

E (eV)	$1s$					$2s$			
	σ_{Ps}^a	σ_{Ps}^b	σ_{Ps}^c	$\sigma_{Ps}^{DWA(HF)}^d$	$\sigma_{Ps}^{DWA}^d$	σ_{Ps}^a	σ_{Ps}^b	σ_{Ps}^c	$\sigma_{Ps}^{DWA}^d$
40	0.4156	0.279	0.568	0.3136	0.3084	0.309[−1]	0.103	0.4688[−1]	0.2404[−1]
60	0.2644		0.358	0.2290	0.2240	0.314[−1]		0.4063[−1]	0.2465[−1]
80		0.1720		0.1376	0.1337	0.169[−1]	0.442[−1]		0.1679[−1]
100	0.955[−1]	0.1080	0.121	0.8193[−1]	0.7915[−1]	0.113[−1]	0.227[−1]	0.1563[−1]	0.1092[−1]
150		0.329[−1]		0.2596[−1]	0.2479[−1]		0.624[−2]		0.3585[−2]
200		0.120[−1]	0.0154	0.1020[−1]	0.9660[−2]		0.182[−2]	0.2038[−2]	0.1419[−2]
500			0.5380[−3]	0.3500[−3]	0.3248[−3]			0.6025[−4]	0.6178[−4]

^aKhan *et al.* [17,18].

^bHewitt *et al.* [19].

^cMandal *et al.* [16].

^dPresent results.

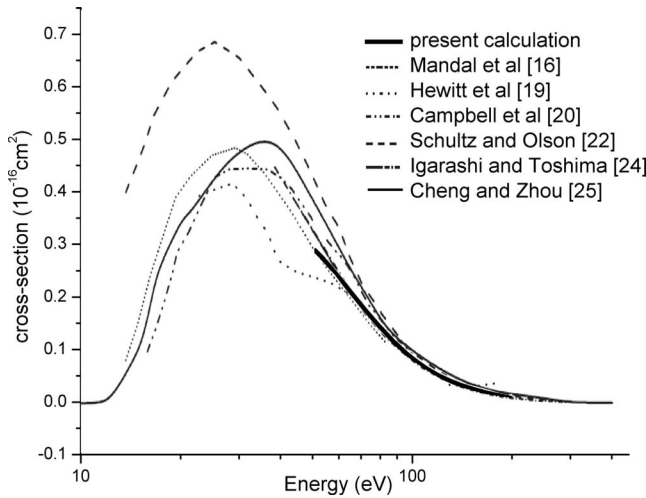


FIG. 1. The present total DWA Ps formation cross section is compared with the available theoretical results.

has been added to 1.66 times the $\text{Ps}(n=2)$ cross section to yield the total Ps formation cross section. We mention here that the $\text{Ps}(2p)$ cross section has been taken from a similar DWA work of Khan *et al.* [17,18].

The total DWA cross sections as obtained thus are compared in Fig. 1 in the energy range of 60–200 eV with the available theoretical calculations of Mandal *et al.* [16], Hewitt *et al.* [19], Campbell *et al.* [20], Schultz and Olson [22], Igarashi and Toshima [24], and Zhou *et al.* [25]. Between 30 and 60 eV, our results are inaccurate and are lower than all the other theoretical values except those of Hewitt *et al.* Beyond 60 eV, there is an overall agreement between all the theoretical cross sections.

Figure 2 shows the comparison of the DWA results in the energy range 60–250 eV with the observed data of Charlton *et al.* [27], Fornari *et al.* [28], Diana *et al.* [28], Fromme *et al.* [29], Murtagh *et al.* [30], and Overton *et al.* [31]. In this figure, we have also included the theoretical results of Zhou *et al.* [25]. It is apparent from this figure that below 60 eV, our DWA cross sections are smaller than all the experimental

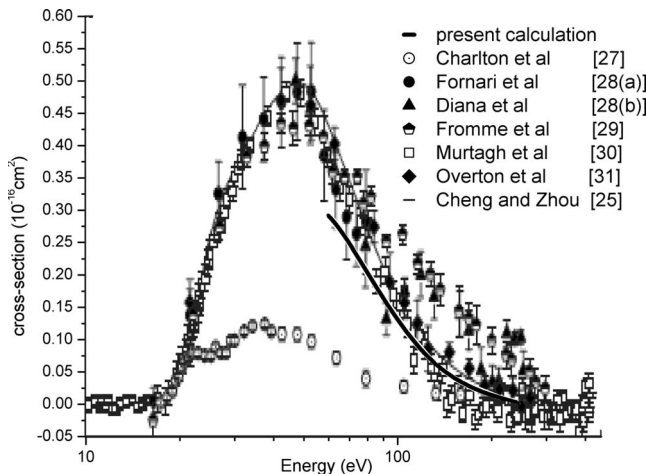


FIG. 2. The present total DWA Ps formation cross section is compared with the available experimental results.

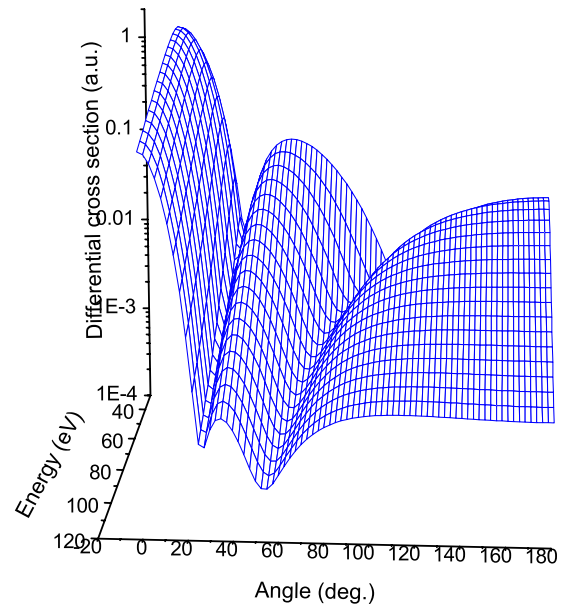


FIG. 3. (Color online) DWA differential cross section (a.u.) for $\text{Ps}(1s)$ formation as a function of incident energy in the range of 30–120 eV and scattering angle in the range of 0° – 180° .

data. However beyond 60 eV, the present DWA results are in agreement with the data of Fornari *et al.*, Diana *et al.* and Murtagh *et al.* It seems that all the observed data are in overall agreement with one another at relatively higher energies beyond 100 eV, in which region the theoretical predictions of Zhou *et al.* and the present calculation are in conformity.

B. Differential cross sections

The DWA differential cross section for $\text{Ps}(1s)$ and $\text{Ps}(2s)$ formations in positron-helium collisions shows dramatic structures. We have endeavored to highlight these structures through surface plots at various orientations.

1. $\text{Ps}(1s)$ formation

In Fig. 3 we display the nature of the differential cross section for the entire scattering angles of 0° – 180° for energy values of 30–120 eV. This figure is very rich in structure and display sharp maxima and minima. It shows primary and secondary critical angles, at which the differential cross section becomes a minimum at any incident positron energy. In general, the differential cross section rises from these critical angles.

The reason for appearance of the critical angles in Ps formation differential cross section is well understood [33,34]. Near a critical angle the lower-partial-wave contributions to the DWA scattering amplitude interfere destructively to show a minimum in the differential cross section, while near a maximum the higher angular momentum states of the scattered Ps interfere constructively. At the critical angle the probability of electron transfer to form the Ps is the lowest for a given incident energy. The present investigations indicate that there exist primary and secondary critical angles in the differential cross section.

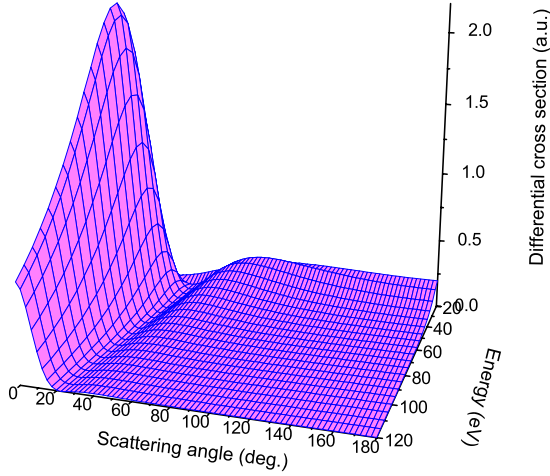


FIG. 4. (Color online) FBA differential cross section (a.u.) for Ps(1s) formation as a function of incident energy in the range of 20–120 eV and scattering angle in the range of 0° – 180° .

While studying the basic nature of the Ps formation differential cross section we have endeavored to see the minimum-transfer flow of Ps at different orientations. The minimum-transfer flow of Ps indeed displays the positions of the critical angles in the energy-angle surface of the differential cross section.

The surface plot of the FBA differential cross section for $N=30$ basis terms is shown in Fig. 4. In this case, we ought to remember that the scattering amplitude becomes exactly zero at an intermediate scattering angle for any incident positron energy due to cancellation of the attractive and repulsive contributions from the residual interaction V_f . This zero moves forward toward 0° with increasing energy. Thus, at such an angle of scattering the probability for Ps formation is exactly nil according to the FBA.

It is also quite interesting to see the nature of the differential cross section at fixed scattering angles as a function of the incident energy. In Fig. 6, we show the behavior of the same at four scattering angles $\theta^\circ=0^\circ, 30^\circ, 60^\circ$, and 90° in the energy range of 30–150 eV.

2. Ps(2s) formation

The differential cross section for Ps(2s) formation has been very seldom studied. Using the simplest Hylleraas wave function for helium, the DWA calculation of Khan *et al.* [17,18] reported differential cross section for Ps formation into $n=2s$ and $n=2p$ states at incident energy of 24 eV. They also included the FBA values for the case of $n=2p$ capture in a tabular form. It is found by our present study that the minimum in the DWA differential cross section disappears for all incident positron energies beyond 400 eV.

The surface plot of the DWA differential cross section is displayed in Fig. 5 in the incident energy range 30–120 eV and for scattering angles of 0° – 180° . This figure clearly indicates the minimum-transfer flow of Ps in the differential cross section.

The interesting nature of the differential cross section at fixed scattering angles of $0^\circ, 60^\circ, 90^\circ$, and 120° is displayed

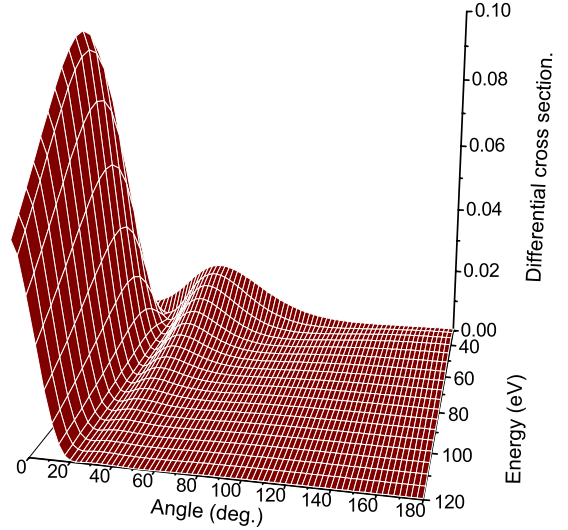


FIG. 5. (Color online) DWA differential cross section (a.u.) for Ps(2s) formation as a function of incident energy in the range of 30–120 eV and scattering angle in the range of 0° – 180° .

in Fig. 7 as a function of energy in the range 30–120 eV. As for Ps(1s) formation, the behavior of the differential cross section in this case also shows some striking features.

IV. CONCLUSIONS

In the present calculation we have used the DWA to predict Ps formation cross sections in $1s$ and $2s$ states in positron-helium collisions at incident positron energies in the range of 30–500 eV. In this work, two points are noteworthy, namely, (i) systematic use of correlated wave function for helium, and (ii) prediction of useful results for Ps formation with the application of a convenient distorted-wave model. DWA calculations are also reported with the use of HF wave function for Ps(1s) formation along with accurate FBA cross sections for Ps(1s) and Ps(2s) formations using upto $N=30$ correlated basis functions.

The present study using DWA reveals for the first time quite a number of interesting features of the differential cross section for Ps formation during positron-helium collisions:

(a) Using quite an accurate correlated helium wave function with $N=30$ basis terms, the DWA results indicate the presence of primary and secondary critical angles in the differential cross section. After each of these minima, the cross section always rises to some maximum value and then falls off with increasing scattering angle. The reason for appearance for such minima and maxima are also well understood by our study.

(b) A number of surface plots have been displayed to show for the first time the presence of rich structure in the differential cross section.

(c) Accurate FBA differential cross sections have been predicted to become zero at intermediate scattering angle. This FBA zero and the DWA primary minimum in the differential cross section always move forward toward 0° with increasing positron energy.

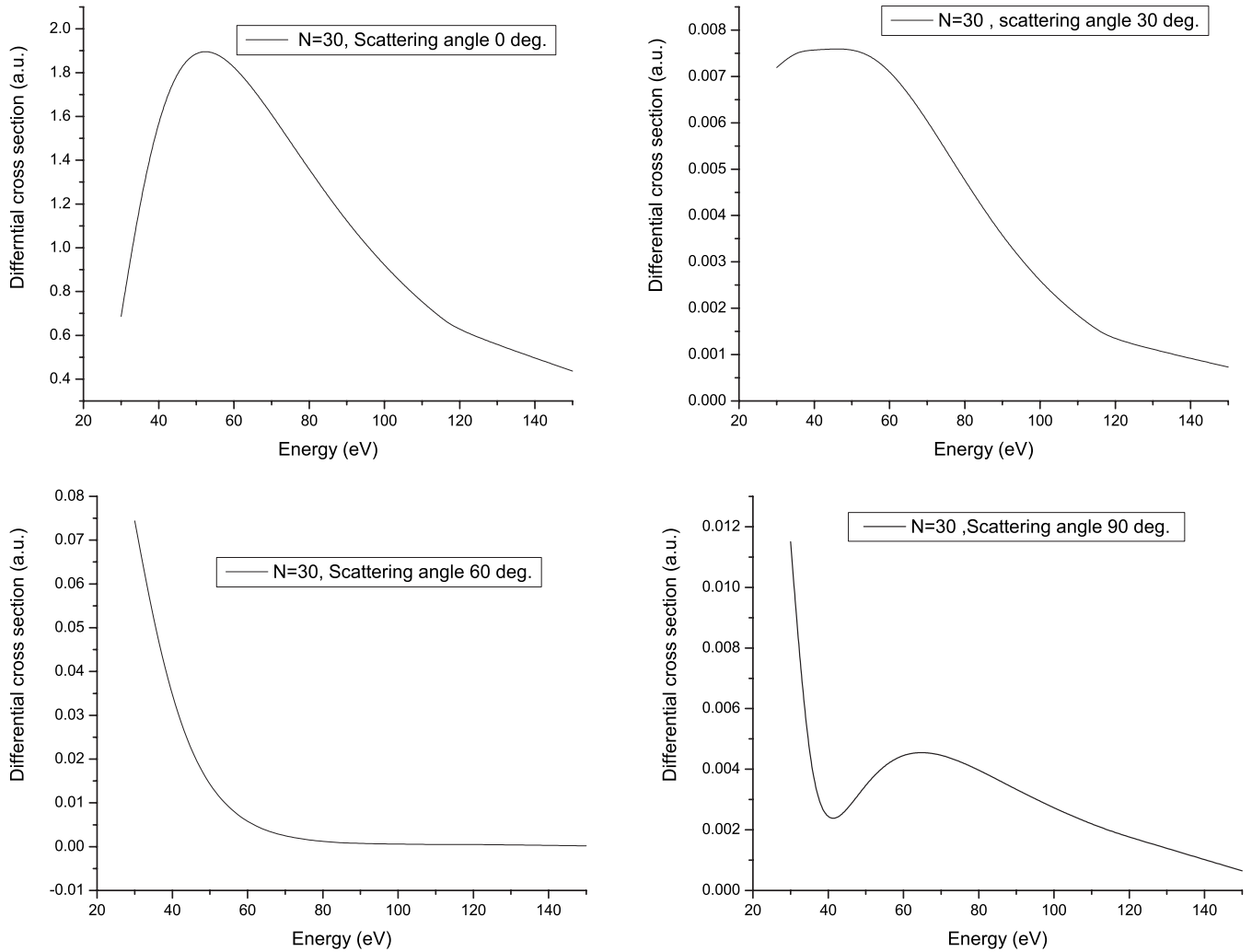


FIG. 6. DWA differential cross section (a.u.) for Ps(1s) as a function of energy in the range of 30–150 eV for the scattering angles of 0°, 30°, 60°, and 90°.

In conclusion, the predicted results for the total Ps formation cross sections within the frame work of DWA are in reasonable agreement with the available theoretical and experimental results beyond incident positron energy of 60 eV, in which $N=30$ correlated basis functions have been included. The agreement is not so good at low energies where the total Ps formation cross section shows a maximum. The reason for that is believed to be an inadequate consideration of the dipole polarization in the incident channel.

Considering all aspects, it may therefore seem to establish the fact that the present application of DWA with exponential correlated helium wave functions is a viable model for prediction of rearrangement scattering processes in positron-helium collisions at intermediate and high energies.

ACKNOWLEDGMENTS

The authors are thankful to the University Grants Commission (UGC), New Delhi for providing funds under its Special Assistance Programme (SAP)–DRS (Phase I) to the Department of Mathematics, Visva-Bharati under Grant No.

F.510/8/DRS/2004(SAP-I). They are also indebted to Professor Y. Zhou for providing with numerical data of her calculations.

APPENDIX: EVALUATION OF U_f FOR POSITRON-HELIUM COLLISIONS

The static potential U_f in exit channel in $e^+ - \text{He}$ collisions is given in a.u. by

$$U_f = \int |\varphi_{\text{He}^+}(\mathbf{r}_2)|^2 |\eta_f(\mathbf{r}_{01})|^2 V_f d\mathbf{r}_{01} d\mathbf{r}_2 \quad (\text{A1})$$

$$= \int |\eta_f(\mathbf{r}_{01})|^2 d\mathbf{r}_{01} \left[\left(\frac{Z}{r_0} - \frac{Z}{r_1} \right) \int |\varphi_{\text{He}^+}(\mathbf{r}_2)|^2 d\mathbf{r}_2 + \int \left(\frac{1}{r_{12}} - \frac{1}{r_{02}} \right) |\varphi_{\text{He}^+}(\mathbf{r}_2)|^2 d\mathbf{r}_2 \right], \quad (\text{A2})$$

where $\eta_f(\mathbf{r}_{01}) = N_f \exp(-\lambda_f r_{01})$, $N_f = \sqrt{\lambda_f^3/\pi}$ and $\varphi_{\text{He}^+}(\mathbf{r}_2) = N_{\text{He}^+} \exp(-\lambda_{\text{He}^+} r_2)$, $N_{\text{He}^+} = \sqrt{\lambda_{\text{He}^+}^3/\pi}$ with $\lambda_f = 1/2$ and $\lambda_{\text{He}^+} = 2$.

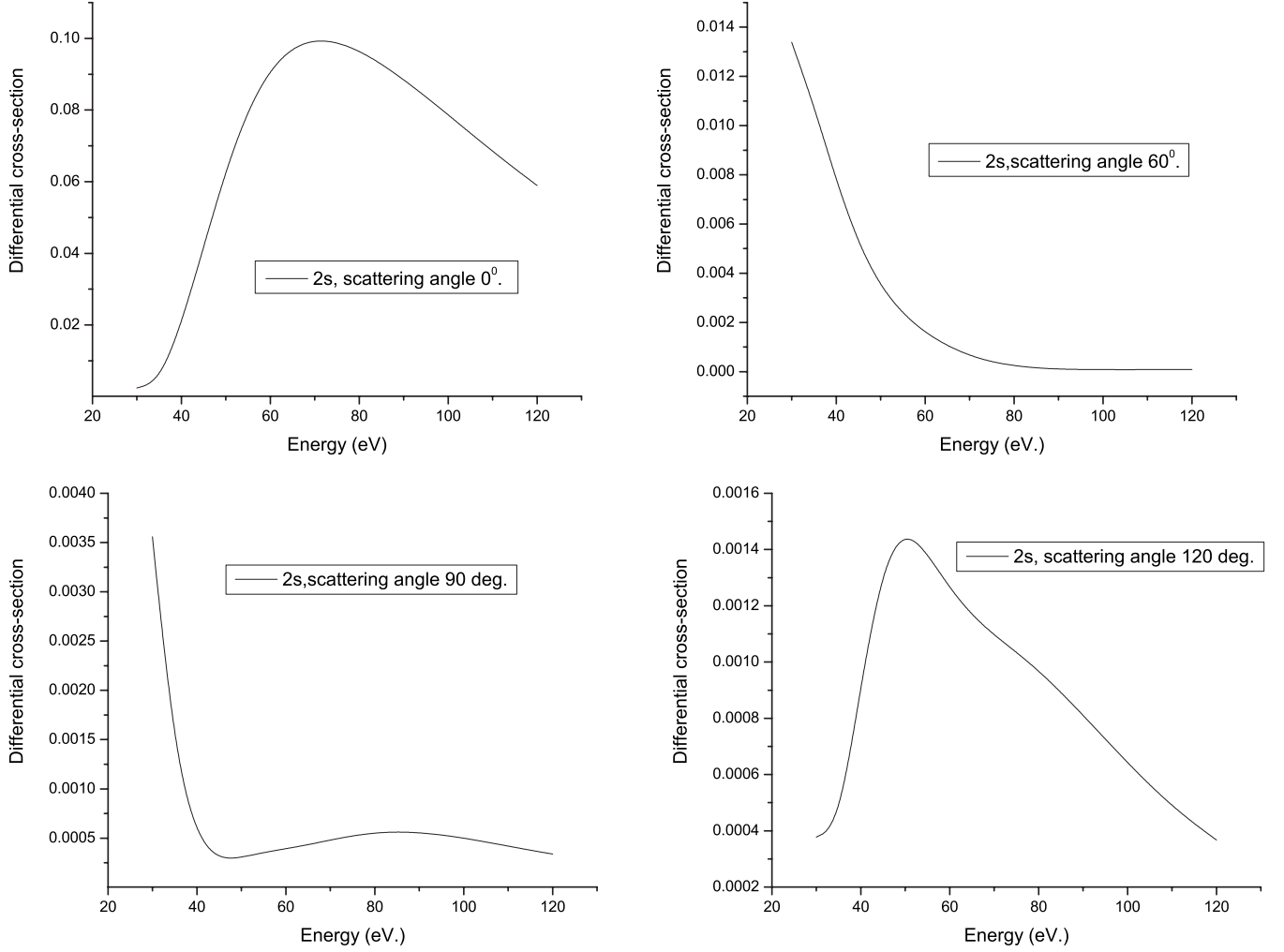


FIG. 7. DWA differential cross section (a.u.) for Ps(2s) as a function of energy in the range of 30–120 eV for the scattering angles of 0°, 60°, 90°, and 120°.

Using $\int |\varphi_{\text{He}^+}(\mathbf{r}_2)|^2 d\mathbf{r}_2 = 1$ and $\mathbf{s} = \mathbf{s}_{01}$ in the first term above, we obtain

$$\begin{aligned}
 U_f &= N_f^2 \int \exp(-2\lambda_f r_{01}) d\mathbf{r}_{01} \left[Z \left(\frac{1}{\left| \mathbf{s} + \frac{1}{2} \mathbf{r}_{01} \right|} - \frac{1}{\left| \mathbf{s} - \frac{1}{2} \mathbf{r}_{01} \right|} \right) \right. \\
 &\quad \left. + N_{\text{He}^+}^2 \int \left(\frac{1}{r_{12}} - \frac{1}{r_{02}} \right) \exp(-2\lambda_{\text{He}^+} r_2) d\mathbf{r}_2 \right] \\
 &= z N_f^2 I_1 + N_{\text{He}^+}^2 (I_2 - I_3),
 \end{aligned} \tag{A3}$$

and

$$\begin{aligned}
 I_2 &= \int \exp(-\beta r_{01}) \exp(-\mu r_2) \frac{1}{r_{12}} d\mathbf{r}_{01} d\mathbf{r}_2 \\
 &= \int \exp(-\beta r_{01}) J_1 d\mathbf{r}_{01},
 \end{aligned} \tag{A5}$$

$$\begin{aligned}
 I_3 &= \int \exp(-\beta r_{01}) \exp(-\mu r_2) \frac{1}{r_{02}} d\mathbf{r}_{01} d\mathbf{r}_2 \\
 &= \int \exp(-\beta r_{01}) J_2 d\mathbf{r}_{01},
 \end{aligned} \tag{A6}$$

where

$$I_1 = \int \exp(-\beta r_{01}) \left(\frac{1}{\left| \mathbf{s} + \frac{1}{2} \mathbf{r}_{01} \right|} - \frac{1}{\left| \mathbf{s} - \frac{1}{2} \mathbf{r}_{01} \right|} \right) d\mathbf{r}_{01}, \tag{A4}$$

with $\beta = 2\lambda_f$ and $\mu = 2\lambda_{\text{He}^+}$.

$$J_1 = \int \exp(-\mu r_2) \frac{1}{r_{12}} d\mathbf{r}_2, \tag{A7}$$

$$J_2 = \int \exp(-\mu r_2) \frac{1}{r_{02}} d\mathbf{r}_2, \tag{A8}$$

Utilizing Fourier integral transforms for functions of the form, $\exp(-\lambda r)/r$, $\exp(-\lambda r)$,

$$\exp(-\lambda r)/r = \frac{1}{2\pi^2} \int \frac{e^{i\mathbf{p}\cdot\mathbf{r}}}{p^2 + \lambda^2} d\mathbf{p},$$

$$\exp(-\lambda r) = \frac{\lambda}{\pi^2} \int \frac{e^{i\mathbf{p}\cdot\mathbf{r}}}{(p^2 + \lambda^2)^2} d\mathbf{p},$$

and the δ -function properties, we get

$$J_1 = 4\pi \frac{\partial}{\partial \mu} \frac{1}{\mu^2} \left(\frac{e^{-\mu r_1}}{r_1} - \frac{1}{r_1} \right), \quad (\text{A9})$$

$$J_2 = 4\pi \frac{\partial}{\partial \mu} \frac{1}{\mu^2} \left(\frac{e^{-\mu r_0}}{r_0} - \frac{1}{r_0} \right), \quad (\text{A10})$$

$$\begin{aligned} I_1 &= \frac{\beta}{2\pi^2} \left[\int \frac{e^{i\mathbf{p}\cdot\mathbf{r}_{01} + i\mathbf{q}\cdot[\mathbf{s} + (1/2)\mathbf{r}_{01}]} }{(p^2 + \beta^2)^2 q^2} d\mathbf{p} d\mathbf{q} d\mathbf{r} \right. \\ &\quad \left. - \int \frac{e^{i\mathbf{p}\cdot\mathbf{r}_{01} + i\mathbf{q}\cdot[\mathbf{s} - (1/2)\mathbf{r}_{01}]} }{(p^2 + \beta^2)^2 q^2} d\mathbf{p} d\mathbf{q} d\mathbf{r} \right] \\ &= \frac{\beta}{2\pi^4} (2\pi)^3 \int \frac{e^{i\mathbf{q}\cdot\mathbf{s}}}{q^2} d\mathbf{q} \left[\frac{1}{\left(\frac{1}{4}q^2 + \beta^2\right)^2} - \frac{1}{\left(\frac{1}{4}q^2 + \beta^2\right)^2} \right] = 0. \end{aligned} \quad (\text{A11})$$

Substituting Eq. (A9) in Eq. (A5), we obtain

$$\begin{aligned} I_2 &= 4\pi \frac{\partial}{\partial \mu} \frac{1}{\mu^2} \int e^{-\beta r_{01}} \left(\frac{e^{-\mu r_1}}{r_1} - \frac{1}{r_1} \right) \\ &= C_3 \frac{\partial}{\partial \mu} \frac{1}{\mu^2} \left[\int \frac{e^{i\mathbf{q}\cdot\mathbf{s}} d\mathbf{q}}{\left(\frac{q^2}{4} + \beta^2\right)^2 (q^2 + \mu^2)} - \int \frac{e^{i\mathbf{q}\cdot\mathbf{s}} d\mathbf{q}}{\left(\frac{q^2}{4} + \beta^2\right)^2 q^2} \right], \end{aligned} \quad (\text{A12})$$

where $C_3 = 4\pi \frac{1}{2\pi^2} \frac{\beta}{\pi^2} \cdot 2\pi^3$

$$I_3 = C_3 \frac{\partial}{\partial \mu} \frac{1}{\mu^2} \left[\int \frac{e^{i\mathbf{q}\cdot\mathbf{s}} d\mathbf{q}}{\left(\frac{q^2}{4} + \beta^2\right)^2 (q^2 + \mu^2)} - \int \frac{e^{i\mathbf{q}\cdot\mathbf{s}} d\mathbf{q}}{\left(\frac{q^2}{4} + \beta^2\right)^2 q^2} \right] \quad (\text{A13})$$

A close look at the terms at once reveals that I_2 and I_3 are identical. Therefore, using Eqs. (A11)–(A13) in Eq. (A3), we get

$$U_f = 0 \quad (\text{A14})$$

-
- [1] T. S. Stein and W. E. Kauppila, *Adv. At. Mol. Phys.* **18**, 53 (1982).
- [2] A. S. Ghosh, N. C. Sil, and P. Mandal, *Phys. Rep.* **87**, 313 (1982).
- [3] M. Charlton, *Rep. Prog. Phys.* **48**, 737 (1985); M. Charlton and G. Laricchia, *J. Phys. B* **23**, 1045 (1990); G. Laricchia and M. Charlton, in *Positron Beams and Their Applications*, edited by P. G. Coleman (World Scientific, Singapore, 2000), p. 41.
- [4] M. Kimura, O. Sueoka, A. Hamada, and Y. Itikawa, *Adv. Chem. Phys.* **111**, 537 (2000).
- [5] M. Charlton and J. W. Humberston, *Positron Physics* (Cambridge University Press, New York, 2001).
- [6] *New Directions in Antimatter Chemistry and Physics*, edited by C. M. Surko and F. A. Gianturco (Kluwer Academic, Dordrecht, 2001).
- [7] L. Spruch and L. Rosenberg, *Phys. Rev.* **117**, 143 (1960); C. Schwartz, *ibid.* **124**, 1468 (1961); R. L. Armstead, *ibid.* **171**, 91 (1968); A. K. Bhatia *et al.*, *Phys. Rev. A* **3**, 1328 (1971); A. K. Bhatia *et al.*, *ibid.* **9**, 219 (1974); D. Register and R. T. Poe, *Phys. Lett.* **51A**, 431 (1975); J. W. Humberston, *Can. J. Phys.* **60**, 591 (1982); *Adv. At. Mol. Phys.* **22**, 1 (1986).
- [8] B. J. Archer, G. A. Parker, and R. T. Pack, *Phys. Rev. A* **41**, 1303 (1990); A. M. Frolov, *ibid.* **60**, 2834 (1999); S. P. Merkuriev *Ann. Phys. (N.Y.)* **130**, 395 (1980); K. Higgins, P. G. Burke, and H. R. J. H. Walters, *J. Phys. B* **23**, 1345 (1990); K. Higgins and P. G. Burke, *ibid.* **24**, L343 (1991); **26**, 4269 (1993); R. Shakeshaft and J. M. Wadehra, *Phys. Rev. A* **22**, 968 (1980); S. J. Ward and J. H. Macek, and S. Yu Ovchinnikov, *Abstracts Positron Workshop on Low-energy Positron and Positronium Physics* (Nottingham University, England, 1997); J. H. Macek and S. Y. Ovchinnikov, *Phys. Rev. A* **54**, 544 (1996).
- [9] R. N. Hewitt, C. J. Noble, and B. H. Bransden, *J. Phys. B* **23**, 4185 (1990); J. Mitroy and A. T. Stelbovics *ibid.* **27**, L55 (1994); *Phys. Rev. Lett.* **72**, 3495 (1994); J. Mitroy, L. Berge, and A. T. Stelbovics, *ibid.* **73**, 2966 (1994); J. Mitroy and K. Ratnavelu, *J. Phys. B* **28**, 287 (1995); A. Igarashi and N. Toshima, *Phys. Rev. A* **50**, 232 (1994); M. T. McAlinden, A. Kernoghan, and H. R. J. Walters, *Hyperfine Interact.* **89**, 161 (1994); T. Gien, *J. Phys. B* **27**, L25 (1994); **28**, 103 (1995); G. Liu and T. T. Gien, *Phys. Rev. A* **46**, 3918 (1992); **49**, 5157(E) (1994); T. T. Gien and G. G. Liu, *ibid.* **48**, 3386 (1993); Y. R. Kuang and T. T. Gien, *ibid.* **55**, 256 (1997).
- [10] B. C. Saha and P. K. Roy, *Phys. Rev. A* **30**, 2980 (1984); D. Basu, G. Banerji, and A. S. Ghosh, *ibid.* **13**, 1381 (1976); M. Basu, M. Mukherjee, and A. S. Ghosh, *J. Phys. B* **22**, 2195 (1989); N. C. Sil, B. C. Saha, H. P. Saha, and P. Mandal, *Phys. Rev. A* **19**, 655 (1979); U. Roy and P. Mandal, *J. Phys. B* **22**, L261 (1989); **23**, L55 (1990); *Phys. Rev. A* **48**, 2952 (1993); S. Kar and P. Mandal, *J. Phys. B* **30**, L627 (1997); **32**, 2297

- (1999); Phys. Rev. A **59**, 1913 (1999); J. Phys. B **33**, L165 (2000).
- [11] G. O. Jones, M. Charlton, J. Slevin, G. Laricchia, A. Kover, M. R. Poulsen, and S. N. Chormaic, J. Phys. B **26**, L483 (1993); J. Moxom, G. Laricchia, and M. Charlton, *ibid.* **28**, 1331 (1995); J. Moxom, P. Ashley, and G. Laricchia, Can. J. Phys. **74**, 367 (1996); S. Zhou, H. Li, W. E. Kauppila, C. K. Kwan, and T. S. Stein, Phys. Rev. A **55**, 361 (1997); W. Sperber, D. Becker, K. G. Lynn, W. Raith, A. Schwab, G. Sinapius, G. Spicher, and M. Weber, Phys. Rev. Lett. **68** 3690 (1992); M. Weber, A. Hofmann, W. Raith, W. Sperber, F. Jacobson, and K. G. Lynn, Hyperfine Interact. **89**, 221 (1994).
- [12] H. S. W. Massey and C. B. O. Mohr, Proc. Phys. Soc., London, Sect. A **67**, 695 (1954).
- [13] H. S. W. Massey and A. H. A. Moussa, Proc. Phys. Soc. London **77**, 811 (1961).
- [14] P. Van Reeth and J. W. Humberston, J. Phys. B **32**, 3651 (1999); J. W. Humberston, *ibid.* **6**, L305 (1973); P. Van Reeth and J. W. Humberston, *ibid.* **32**, L103 (1999); J. T. Dunn, J. W. Humberston, and P. Van Reeth, *ibid.* **35**, 5153 (2002).
- [15] P. Mandal, A. S. Ghosh, and N. C. Sil, J. Phys. B **8**, 2377 (1975); P. Mandal, D. Basu, and A. S. Ghosh, *ibid.* **9**, 2633 (1976).
- [16] P. Mandal, S. Guha, and N. C. Sil, J. Phys. B **12**, 2913 (1979); Phys. Rev. A **22**, 2623 (1980).
- [17] P. Khan and A. S. Ghosh, Phys. Rev. A **28**, 2181 (1983).
- [18] P. Khan, P. S. Mazumdar, and A. S. Ghosh, Phys. Rev. A **31**, 1405 (1985).
- [19] R. N. Hewitt, C. J. Noble, and B. H. Bransden, J. Phys. B **25**, 557 (1992).
- [20] C. P. Campbell, M. T. McAlinden, A. Kernoghan, and H. R. J. Walters, Nucl. Instrum. Methods Phys. Res. B **143** 41 (1998).
- [21] H. Wu, I. Bray, D. V. Fursa, and A. T. Stelbovics, J. Phys. B **37**, 1165 (2004).
- [22] D. R. Schultz and R. E. Olson, Phys. Rev. A **38**, 1866 (1988).
- [23] N. C. Deb, D. S. F. Crothers, and D. Fromme, J. Phys. B **23**, L483 (1990).
- [24] A. Igarashi and N. Toshima, Phys. Lett. A **164**, 70 (1992); A. Igarashi *et al.*, Phys. Rev. A **54**, 5004 (1996).
- [25] Y. Cheng and Y. Zhou, Phys. Rev. A **76**, 012704 (2007); **73**, 024701 (2006); Y. Zhou, K. Ratnavelu, and I. E. McCarthy, *ibid.* **71**, 042703 (2005); Y. Ke, Y. Zhou, and G. Nan, *ibid.* **70**, 024702 (2004).
- [26] W. E. Kauppila, T. S. Stein, J. H. Smart, M. S. Dababneh, Y. K. Ho, J. P. Downing, and V. Pol, Phys. Rev. A **24**, 725 (1981).
- [27] M. Charlton, G. Clark, T. C. Griffith, and G. R. Heyland, J. Phys. B **16**, L465 (1983).
- [28] L. S. Fornari, L. M. Diana, and P. G. Coleman, Phys. Rev. Lett. **51**, 2276 (1983); L. M. Diana, P. G. Coleman, D. L. Brooks, P. K. Pendleton, and D. M. Norman, Phys. Rev. A **34**, 2731 (1986).
- [29] D. Fromme, G. Kruse, W. Raith, and G. Sinapius, Phys. Rev. Lett. **57**, 3031 (1986).
- [30] D. J. Murtagh, M. Szluinska, J. Moxom, P. Van Reeth, and G. Laricchia, J. Phys. B **38**, 3857 (2005).
- [31] N. Overton, R. J. Mills, and P. G. Coleman, J. Phys. B **26**, 3951 (1993).
- [32] S. Kar and Y. K. Ho, J. Phys. B **37**, 3177 (2004); Chem. Phys. Lett. **402**, 544 (2005); S. Kar and Y. K. Ho (private communication).
- [33] A. Ghoshal and P. Mandal, Phys. Rev. A **72**, 032714 (2005); J. Phys. B **41**, 175203 (2008).
- [34] A. Ghoshal and P. Mandal, Phys. Rev. A **72**, 042709 (2005); **72**, 042710 (2005).